Title

Rates of Retinal Nerve Fiber Layer Thinning in Distinct Glaucomatous Optic Disc Phenotypes in Early Glaucoma

Authors

David, Ryan Caezar C
Moghimi, Sasan
Ekici, Eren
et al.

Publication Date

2021-09-01

DOI

10.1016/j.ajo.2021.04.010

Peer reviewed

HHS Public Access

Author manuscript

Am J Ophthalmol. Author manuscript; available in PMC 2022 September 12.

Published in final edited form as:

Am J Ophthalmol. 2021 September ; 229: 8–17. doi:10.1016/j.ajo.2021.04.010.

Rates of RNFL thinning in distinct glaucomatous optic disc phenotypes in early glaucoma

Ryan Caezar C. David, MD[1], **Sasan Moghimi, MD**[1], **Eren Ekici, MD**[1], **Jiun L. Do, MD, PhD**[1], **Huiyuan Hou, MD, PhD**[1], **James A. Proudfoot, MSc**[1], **Alireza Kamalipour, MD**[1], **Takashi Nishida, MD, PhD**[1], **Christopher A. Girkin, MD, MSPH**[2], **Jeffrey M. Liebmann, MD**[3], **Robert N. Weinreb, MD**[1]

[1]Hamilton Glaucoma Center, Shiley Eye Institute, Viterbi Family Department of Ophthalmology, University of California, San Diego, La Jolla, CA, United States.

[2]Department of Ophthalmology and Visual Science, Callahan Eye Hospital, University of Alabama-Birmingham, AL, United States.

[3]Bernard and Shirlee Brown Glaucoma Research Laboratory, Department of Ophthalmology, Edward S. Harkness Eye Institute, Columbia University Medical Center, New York, NY, United States.

Abstract

Purpose: To compare spectral-domain optical coherence tomography (SDOCT) measured circumpapillary retinal nerve fiber layer (cpRNFL) among four glaucomatous optic disc phenotypes in early glaucoma.

Design: Clinical cohort study

Methods: In this study, 218 early glaucoma eyes that had at least 3 years of follow-up and a minimum of 4 SDOCT scans were recruited. The optic discs were classified into four types based on appearance: 76 generalized cup enlargement (GE), 53 focal ischemic (FI), 22 myopic glaucomatous (MY), and 67 senile sclerotic (SS). A linear mixed-effect model was used to compare the rates of global and regional cpRNFL thinning among optic disc phenotypes.

Results: After adjusting for confounders, the SS group (mean (95% CI): −1.01 (−1.30, −0.73) μm/year) had the fastest mean rate of global cpRNFL thinning followed by FI (−0.77 (−0.97, −0.57) μm/year), MY (0.59 (−0.81, −0.36) μm/year) and GE (−0.58 (−0.75, −0.40) μm/year) at p<0.001. The inferior temporal sector had the fastest rate of cpRNFL thinning among the regional measurements except for the MY group (−0.68 (−1.10, −0.26) μm/year), p=0.002). In

Corresponding author: Robert N. Weinreb, MD, Shiley Eye Institute, University of California, San Diego, 9500 Campus Point Drive, La Jolla, CA, 92093-0946, rweinreb@health.ucsd.edu.

Financial Disclosures: C.A.G.: Research support: Heidelberg Engineering, GmbH, Heidelberg, Germany. **J.M.L.:** Consultant: Sensimed Inc., Lausanne, Switzerland; Carl Zeiss Meditec, Jena, Germany, Inc.; Alcon Laboratories, Fort Worth, TX; Topcon Inc., Tokyo, Japan; Heidelberg Engineering, GmBH, Heidelberg, Germany; Allergan Inc., Dublin, Ireland; Bausch & Lomb Inc., Garden City, NY; Aerie Pharmaceuticals Inc., Pittsburgh, PA; Quark Pharmaceuticals Inc., Ness Ziona, Israel. **R.N.W.:** Financial support: Carl Zeiss Meditec Inc., Jena, Germany; Heidelberg Engineering, GmbH, Heidelberg, Germany; Optovue Inc., Fremont, CA; Topcon Medical Systems, Tokyo, Japan. Grants: Quark Pharmaceuticals Inc., Ness Ziona, Israel; Genentech—San Francisco, CA. Consultant: Aerie Pharmaceuticals, Pittsburgh, PA; Alcon Laboratories Inc., Fort Worth, TX; Allergan Inc., Dublin, Ireland; Bausch & Lomb, Garden City, NY. The remaining authors declare no conflict of interest.

the multivariable analysis, GE (p=0.002) and MY (p=0.010) phenotypes were associated with significantly slower global rates of cpRNFL thinning when compared to the SS phenotype.

Conclusions: Rates of cpRNFL thinning were different among the four glaucomatous optic disc phenotypes. Those patients with early glaucoma with SS phenotype have the fastest cpRNFL thinning. These patients may benefit from more frequent monitoring and the need to advance therapy if cpRNFL thinning is detected.

Keywords

retinal nerve fiber layer; optic disc phenotypes; glaucoma; progression

Introduction

Glaucoma is an optic neuropathy characterized by progressive structural changes, loss of retinal ganglion cells (RGCs) and their axons, and damage to the visual field (VF).[1, 2] The chronic and progressive nature of glaucoma requires timely detection of the disease through analysis of structural and functional changes. Optical coherence tomography (OCT) quantifies structural parameters of the optic disc and circumpapillary retinal nerve fiber layer (cpRNFL) with good precision and reproducibility.[3-5] In early glaucoma, cpRNFL thinning can occur without VF changes and can be detected using OCT.[6] Moreover, faster rate of global cpRNFL loss has been implicated with higher risk of developing visual field defect in glaucoma suspects.[7]

Glaucomatous damage to the optic disc can manifest with different morphological patterns.[8] It has been proposed that certain patterns of optic disc damage are secondary to specific pathophysiological mechanisms and patients can be categorized into four clinical subtypes based on the appearance of the optic nerve.[9, 10] Morphological subtypes of glaucomatous optic disc damage may therefore help to differentiate the wide clinical spectrum of open-angle glaucoma.

This study determined patterns of cpRNFL thinning in the four glaucomatous optic disc phenotypes of patients with early glaucoma followed prospectively for several years.

Methods

This was an observational cohort study in participants from a prospective longitudinal study designed to evaluate optic nerve structure and visual function in glaucoma (Diagnostic Innovations Glaucoma Study [DIGS] and African Descent and Glaucoma Evaluation Study [ADAGES]).[11] Participants in these cohorts were longitudinally evaluated according to a pre-established protocol that included regular follow-up visits in which patient underwent a clinical examination, imaging, and functional tests. All participants from the DIGS and ADAGES study who met the inclusion criteria described below were enrolled in the current study. Informed consent was obtained from all participants. The University of California, San Diego Human Subject Committee approved all protocols, and the methods described adhered to tenets of the Declaration of Helsinki.

Participants

All patients underwent an annual comprehensive ophthalmologic examination, including best-corrected visual acuity, slit-lamp biomicroscopy, Goldmann applanation tonometry, gonioscopy, dilated fundus examination, stereoscopic optic disc photography, ultrasound pachymetry, and standard automated perimetry (SAP) in both eyes. Semi-annual examinations included intraocular pressure (IOP) measurement, spectral-domain optical coherence tomography (SDOCT) imaging, and SAP testing.

Glaucoma was defined as the presence of glaucomatous optic nerve damage (i.e., the presence of focal thinning, notching, or localized or diffuse atrophy of the RNFL) with a reliable (fixation losses <33%, false negatives <33% and false positives <33%) and repeatable abnormal SAP tests using the 24-2 Swedish Interactive Threshold Algorithm with either a Pattern Standard Deviation outside the 95% normal limits or a Glaucoma Hemifield Test result outside the 99% normal limits. Patients with baseline 24-2 mean deviation (MD) >−6.0 dB were included in this study.

Inclusion criteria included (1) older than 18 years of age, (2) open angles on gonioscopy, (3) best-corrected visual acuity of 20/40 or better and (4) at least 3 years of follow-up with a minimum of 4 SDOCT scanning sessions.

Exclusion criteria included (1) history of trauma or intraocular surgery (except for uncomplicated cataract surgery or glaucoma surgery), (2) coexisting retinal disease, (3) uveitis, or (4) non-glaucomatous optic neuropathy. Participants with the diagnosis of Parkinson’s disease, Alzheimer’s disease, dementia, or a history of stroke were also excluded. Those with unreliable visual fields (VFs) or poor-quality SDOCT scans were also excluded from this report.

Optic Disc Classification

All color simultaneous stereophotographs were taken using a Nidek Stereo Camera Model 3-DX (Nidek Inc, Palo Alto, CA) after maximal pupil dilation. All photograph evaluations were performed using a simultaneous stereoscopic viewer (Asahi Pentax Stereo Viewer II; Pentax, Tokyo, Japan) with a standard fluorescent light bulb. As described by Nicolela and Drance[9] and then in our previous study,[12] the optic discs were classified into four types based on appearance: generalized cup enlargement (GE), focal ischemic (FI), myopic glaucomatous (MY), and senile sclerotic (SS). For optic discs with GE, the cup is concentrically enlarged and there are no localized areas of neuroretinal rim loss or pallor. For focal optic disc damage, the neuroretinal rim has a localized notch inferiorly or superiorly, while the remaining tissue is relatively well preserved. For optic discs classified as the high myopia phenotype, there is a tilted appearance, shallow cupping, and a myopic crescent of peripapillary atrophy. Optic discs with sclerotic damage have shallow cupping with marked areas of peripapillary atrophy. The classification of optic disc phenotype was evaluated by two experienced graders (EE and SM) using a stereoscopic viewer. Each grader was masked to the subject’s identity and the other test results. All included photographs were judged to be of adequate quality or better. Discrepancies between the two graders were

resolved by consensus or adjudication by a third experienced grader. Inability to reach a consensus resulted to exclusion of the case.

OCT Measurements

The Spectralis SDOCT (software version 5.4.7.0, Heidelberg Engineering, Inc.) was used to obtain circumpapillary retinal nerve fiber layer (cpRNFL) measurements. Details of its operation have been discussed elsewhere.[13] The high-resolution protocol was used, obtaining 1536 A-scans from a 3.45mm circle centered at the optic disc, providing an axial resolution of 3.9μm and a lateral resolution of 6μm. The Spectralis SDOCT included an automatic real time function that gathers multiple frames (B-scans) to increase image quality. The images were then averaged for noise reduction. The quality score ranges from 0 dB (poor) to 40 dB (excellent). To be included, all images were reviewed by experienced graders of the Imaging Data Evaluation and Assessment (IDEA) Center for non-centered scans, accurate segmentation, and a signal strength > 15dB. The cpRNFL measurements evaluated in this study included the mean global index, temporal quadrant (316 – 45 degrees), superior temporal sector (46 – 90 degrees), superior nasal sector (91 – 135 degrees), nasal quadrant (136 – 225 degrees), inferior nasal sector (226 – 270 degrees) and inferior temporal sector (271 – 315 degrees).

Statistical analysis

Descriptive statistics were calculated as the mean and 95% confidence interval (95% CI). Categorical variables were compared using the chi-square test. The kappa value was used to estimate the extent of agreement between the 2 observers. Mixed-effects modeling was used to compare ocular parameters among groups. Models were fitted with ocular measurements as response variable and classification groups as fixed effects. Measurements of bilateral eyes were nested within subject to account for the fact that eyes from the same individual were more likely to have similar measurements. Contributory factors affecting cpRNFL thinning were examined using a univariable and multivariable linear mixed model. Multivariable models were constructed including the following potential confounding factors: age, gender, baseline 24-2 mean deviation (MD) and any other ocular parameters in which the p value was <0.1 in univariable analysis.

The evaluation of the effect of optic disc phenotype parameters on mean rates of change in cpRNFL in each group were performed using a linear mixed model with random intercepts and random slopes.[14-16] In this model, the average evolution of the outcome variable (cpRNFL measurements) was explored using a linear function of time, and random intercepts and random slopes were introduced with patient- and eye-specific deviations from this average evolution. The model can account for the fact that different eyes can have different rates of cpRNFL thinning over time, while accommodating correlations between both eyes of the same individual.[14, 15] Because cpRNFL decline may depend on disease severity, an unstructured covariance between random effects was assumed, allowing for correlation between intercepts and slopes of change.[17] In addition to putative predictors to examine the effect of variables on the baseline cpRNFL, interaction terms between time and predictors were included in the model to explore whether there is a significant effect of the predictor on changes of the outcome variable over time. Age, race, baseline 24-2 MD, and

mean IOP during follow-up were used as predictors in this investigation. In the evaluation of progressors, individual slopes in each phenotype were classified into groups according to pre-established range for mean rates of global cpRNFL thinning: slow, if change was greater than −1.0 μm/year; moderate, if between −1.0 to −2.0 μm/year; and fast, if change was less than −2.0 μm/year.[18]

All statistical analyses were performed with commercially available software (Stata version 14; StataCorp, College Station, Texas, USA). Statistical significance for tests was set at $p \leq 0.05$.

Results

Overall, 218 eyes from 173 glaucoma subjects met our inclusion criteria and were enrolled in this longitudinal study. Of these eyes, the optic disc appearance of 76 eyes were classified as generalized cup enlargement (GE), 53 eyes as focal ischemic (FI), 22 eyes as myopic glaucomatous (MY), and 67 eyes as senile sclerotic (SS). The kappa value for interobserver agreement in classification into the 4 types of glaucomatous optic disc phenotypes was good at 0.833 (95% CI: 0.807 - 0.840).

The baseline demographics of the subjects with GE, FI, MY, and SS groups, are summarized in Table 1. The mean baseline age of the SS group (74.3 years) was the oldest compared to the other 3 groups (p=0.001). The GE group was predominantly of African American descent (54.1%, p=0.001). The incidence of self-reported diabetes mellitus was higher in the GE (29.5%) especially when compared to FI and MY groups (p=0.004). The MY group had a longer mean axial length (AL) among the groups and was statistically significant when compared to GE and FI groups (p=0.051). Baseline 24-2 MD was higher in the GE and MY groups compared to SS and FI groups (p<0.001). Similarly, the GE and MY groups had statistically significant thicker baseline global cpRNFLs when compared to FI and SS groups (p<0.001). The SS group had higher central corneal thickness measurements among phenotypes and was statistically significant when compared to GE group (p=0.160). Other variables including baseline IOP, mean IOP during follow-up, follow-up time and number of OCT follow-up scans were comparable among phenotype groups.

SDOCT measurements, including global and regional rates of cpRNFL thinning are presented in Table 2. The difference in the global rate of cpRNFL thinning were statistically significant between optic disc phenotypes (p<0.001). SS group (mean (95% CI): −1.01 (−1.30, −0.73) μm/year) had the fastest mean rate of global cpRNFL thinning followed by FI (−0.77 (−0.97, −0.57) μm/year), MY (0.59 (−0.81, −0.36) μm/year) and GE (−0.58 (−0.75, −0.40) μm/year). The inferior temporal sector had the fastest rate of cpRNFL thinning among other regional measurements in most groups except for MY group (−0.68 (−1.10, −0.26) μm/year), p=0.002). Temporal and nasal quadrants were the least affected in all phenotypes. However, in pairwise comparison, the SS group (−0.76 (−1.05, −0.47) μm/year) had statistically significant faster rate of cpRNFL thinning in the temporal quadrant when compared to GE (−0.20 (−0.37, −0.04) μm/year) and FI (−0.20 (−0.50, 0.11) μm/year) groups at p<0.05. After adjustments for age, race, 24-2 MD at baseline, and mean IOP during follow-up, the results were similar. Figure 1 depicts the estimated

mean rates of global and regional cpRNFL thinning in each glaucomatous optic disc phenotype. Furthermore, the SS and FI groups had higher proportion of both moderate to fast progressors compared to other phenotypes (p=0.015). The frequency of eyes in each phenotype classified as slow, moderate, and fast progressors according to the previously determined range is shown in Figure 2.

Factors contributing to the rate of cpRNFL thinning among the subjects are shown in Table 3. In the multivariable analysis, higher mean IOP during follow-up (p<0.001) and optic disc phenotype (p=0.014) were associated with increased cpRNFL thinning. The GE (p=0.002) and MY (p=0.010) phenotypes were also associated with statistically significant slower rates of cpRNFL thinning when compared to SS phenotype.

Discussion

In this study, glaucomatous optic disc phenotypes were associated with the rates of cpRNFL thinning in early glaucoma patients. Senile sclerotic (SS) and focal ischemic (FI) phenotypes showed faster rates of global cpRNFL thinning compared to generalized cup enlargement (GE) and myopic glaucomatous (MY) phenotypes. Characteristic patterns of cpRNFL thinning were also seen in each group. These findings suggest that the assessment and classification of optic nerve head phenotypes may enhance the evaluation of the risks and behavior of glaucoma structural progression.

Development and progression of primary open angle glaucoma (POAG) is likely dependent on the risk factors of an individual patient. Several risk factors were associated with certain optic disc phenotypes. SS phenotypes are associated with older age and several systemic risk factors.[10] Various studies suggest that age is an independent risk factor for both the prevalence[19] and progression of glaucomatous damage.[20-22] The extent of physiologic stress and strain that the ONH connective tissues are exposed to over a lifetime could be related to increased susceptibility of the aged ONH to glaucoma. It has been proposed that senile sclerotic ONHs are more likely to have stiffer connective tissues[23-25] and compromised vasculature[26-28] with an increased susceptibility to damage of the superior and inferior vulnerable regions. In another study comparing lamina cribrosa (LC) depth among phenotypes, LC depth of SS group was notably shallow and similar to that of the healthy group.[29] Furthermore, our recent study on estimated circumpapillary capillary density loss among phenotypes showed a similar pattern of deterioration and concluded that lower vessel density was significantly associated with SS group.[12] In the current study, amidst the appearance of a shallow saucer-shaped cup, the SS group had a distinct faster pattern of deterioration affecting both the superior and inferior vulnerable zones of glaucoma. Moreover, the SS group had the fastest global and regional rates of cpRNFL thinning among phenotypes. We hypothesize that the fast cpRNFL thinning in SS group resulted from combined mechanical and vascular mechanisms present in aged ONHs.

Focal notching of the neuroretinal rim with a corresponding visual field (VF) defect, which threatens fixation early in the disease is described as focal ischemic type of glaucoma.[9, 30, 31] Earlier age of onset, female gender, occurrence of disc hemorrhage and primary vascular dysregulation syndromes (vasospasm, migraine, nocturnal hypotension,

Raynaud's phenomenon) are associated with FI phenotype.[9, 30, 32, 33] Presence of a notch in the optic disc neural rim has been highly associated with glaucoma.[34] Subsequent studies showed the association between focal LC defects and glaucomatous rim narrowing.[35] Impaired vascular supply to the laminar region, either independent of or associated with increased IOP, may be another factor that can lead to structural changes of the LC, weakening the laminar beams and making them prone to collapse.[36, 37] In this study, the FI group showed both rapid focal and global cpRNFL thinning. Inferior quadrant was more affected compared with the superior quadrant involving more of the superior temporal sector only. Monitoring for regional and global glaucomatous progression in the FI phenotype is of great importance due to its characteristic early age of onset, rapid rate of both local and global deterioration, and possible earlier effect on fixation which are all detrimental to vision-related quality of life for patients.

Myopia has been consistently associated with the prevalence of glaucoma. A meta-analysis study by Marcus et al, documented that myopia had a pooled odds ratio of 1.92 for glaucoma.[38] It has been proposed that myopic optic nerve head deformations may increase the predisposition for glaucomatous injury.[39, 40] Myopic eyes with open angle glaucoma exhibited increased quantity of lamina cribrosa defects and large pores at similar locations as those with healthy myopic eyes, suggesting that these focal alternations of the lamina in myopia may develop into larger defects in glaucoma.[41] In the current study, having comparable IOP exposure among groups, the MY group had a slower rate of cpRNFL thinning. These findings suggest that in the myopic glaucoma continuum, lamina cribrosa defects may develop in an IOP-independent process that results in further glaucomatous changes only when exposed to elevated IOP. A study by Sung et al,[42] revealed that the location of RNFL damage was consistent with the direction of optic disc rotation in almost 60% of normal tension glaucoma (NTG) eyes, showing optic disc rotation-VF defect correspondence. In addition, Han et al, also observed that NTG with myopia seems to have a slow VF progression rate even without glaucoma medications.[43] In this study, myopic POAG eyes showed a similar slow rate of glaucomatous progression.

Increased excavation is one of the most commonly described feature among glaucomatous optic nerve changes.[44] Patients with GE are usually associated with higher pretreatment maximal IOP and average IOP during follow-up.[10] Furthermore, eyes with concentric optic disc appearance were evaluated to have significantly higher IOP elevation during the nocturnal period compared to the eyes with non-concentric optic disc appearance.[45] Greater LC depth was also associated with the GE phenotype.[29] It was postulated that glaucomatous damage occurs in this phenotype at a younger age where laminar tissue might have been more compliant. Therefore, posterior deformation ensues prior to initiation of IOP-lowering therapy.[29] In this study, the GE group presented with slower global rate of cpRNFL thinning similar to MY group; however, GE group had a localized inferior pattern of deterioration comparable with the FI group. This may indicate that GE group may have a localized glaucomatous progression even with a slow global rate of cpRNFL progression. In the Ocular Hypertension Treatment Study (OHTS), every 0.1-unit increase in the baseline cup to disc ratio was associated with a 1.4-fold increase in the incidence of POAG among study subjects with ocular hypertension.[20] Interestingly in a study by Nakazawa et al, the GE phenotype was noted to be the predominant form in advanced POAG. It was proposed

that GE is a result of progressive axonal loss in glaucoma.[46] Therefore, whether distinct features of the optic disc such as concentric excavation are congenital variants or the result of progressive axonal loss is unclear. In this study, only pure optic disc phenotypes in early glaucoma were included to increase reliability in the measurement of the different effects of each morphological optic disc features on the rates of cpRNFL thinning. These data suggest that the four optic disc phenotypes may have different mechanisms of injury in producing distinct patterns of cpRNFL thinning.

Unique patterns of structural and functional glaucoma progression among optic disc phenotypes have been described previously.[9, 12, 29, 47-50] In the current study, most phenotypes had their fastest rates of cpRNFL thinning involving the inferior temporal sector followed by the superior temporal sector. These locations have been implicated as vulnerable zones in the disease.[51-53] The temporal and nasal quadrants were less affected by progression among the regions. A study by Takada et al.[54] found that RNFL thinning was significantly more frequent in both the superior and inferior quadrants among phenotypes. Omodaka et al.[50] demonstrated that the region of the disc with the highest correlation coefficient between structure and function differed based on optic disc phenotypes. In this study, phenotypes differed in terms of rates of cpRNFL thinning and patterns of deterioration. The MY and GE phenotypes both had significantly slower global rate of deterioration when compared to SS group. The MY group showed a characteristic slower rate of cpRNFL deterioration in the inferior temporal sector among the phenotypes. In comparison, a more localized inferior cpRNFL thinning was observed in the GE and FI groups. Finally, the SS group had a distinct rapid rate of cpRNFL thinning both in the superior and inferior quadrants. Therefore, in early stages of glaucoma, these patterns of cpRNFL thinning among phenotypes should be analyzed with caution, as some may have rapid localized forms of progression masked by a slow rate of global progression.

After adjusting for optic disc phenotypes, higher mean IOP during follow-up was significantly associated with faster cpRNFL thinning over time in glaucoma subjects. Although IOPs were comparable among the disc phenotype groups, phenotypes had different patterns of cpRNFL thinning. A study that evaluated the association between IOP and cpRNFL loss determined that the rates of cpRNFL deterioration for each mmHg was greater in glaucoma progressors compared to non-progressors, suggesting heterogenous susceptibility to IOP levels.[55] These findings suggest that optic disc phenotypes may be used as surrogate for vulnerability to IOP.

This study has some limitations. First, optic disc phenotype classification was based on subjective observation. To address this limitation, two experienced graders were tasked with classifying optic disc phenotypes and demonstrated good interobserver agreement in determining the final classification ($\kappa = 0.833$). Second, uncontrolled differences in ocular and systemic characteristics between optic disc phenotype groups could affect the cpRNFL measurements. Third, although, the optic discs were classified into four different phenotypes as described by Nicolela and Drance,[9] optic disc appearances with a mixed phenotype are possible and common.[12, 56] Only pure optic disc phenotypes were included in this study. Finally, the diagnosis of glaucoma may have led to the initiation or intensification of

IOP-lowering therapy in disease treatment, potentially decreasing the true effect of distinct phenotypes on the rates of cpRNFL thinning.

In conclusion, this longitudinal study demonstrated different rates of glaucomatous cpRNFL thinning among four distinct optic disc phenotypes. Those patients with early glaucoma and the SS optic disc phenotype have faster cpRNFL thinning. These patients may benefit from more frequent monitoring and the need to advance therapy if cpRNFL thinning is detected.

Acknowledgements

Supported by the National Eye Institute Grants R01EY026574 (**C.A.G**), U10EY010427 (**J.M.L**), and R01EY029058 (**R.N.W**), K12 Career Development Grant (**J.L.D**), Bethesda, MD; Tobacco-Related Disease Research Program T31IP1511 (**S.M.**), Oakland, CA; Eyesight Foundation of Alabama, Birmingham, AL; and an Unrestricted departmental Grant from Research to Prevent Blindness, New York, NY (Department of Ophthalmology, Columbia University Medical Center and Department of Ophthalmology, University of California San Diego).

Abbreviations and Acronyms:

ADAGES	African Descent and Glaucoma Evaluation Study
CCT	central corneal thickness
CI	confidence interval
cpRNFL	circumpapillary retinal nerve fiber layer
DIGS	Diagnostic Innovations in Glaucoma Study
IOP	intraocular pressure
LC	lamina cribrosa
MD	mean deviation
OCT	optical coherence tomography
POAG	primary open angle glaucoma
SDOCT	spectral domain optical coherence tomography
VF	visual field

References

1. Weinreb RN, Leung CK, Crowston JG, et al. Primary open-angle glaucoma. Nat Rev Dis Primers 2016;2:16067. [PubMed: 27654570]
2. Weinreb RN, Aung T, Medeiros FA. The pathophysiology and treatment of glaucoma: a review. JAMA 2014;311:1901–11. [PubMed: 24825645]
3. Blumenthal EZ, Williams JM, Weinreb RN, Girkin CA, Berry CC, Zangwill LM. Reproducibility of nerve fiber layer thickness measurements by use of optical coherence tomography. Ophthalmology 2000;107:2278–82. [PubMed: 11097610]
4. Vessani RM, Moritz R, Batis L, Zagui RB, Bernardoni S, Susanna R. Comparison of quantitative imaging devices and subjective optic nerve head assessment by general ophthalmologists to differentiate normal from glaucomatous eyes. J Glaucoma 2009;18:253–61. [PubMed: 19295383]

5. Hondur G, Goktas E, Al-Aswad L, Tezel G. Age-related changes in the peripheral retinal nerve fiber layer thickness. Clin Ophthalmol 2018;12:401–409. [PubMed: 29520130]
6. Pagliara MM, Lepore D, Balestrazzi E. The role of OCT in glaucoma management. Prog Brain Res 2008;173:139–48. [PubMed: 18929106]
7. Miki A, Medeiros FA, Weinreb RN, et al. Rates of retinal nerve fiber layer thinning in glaucoma suspect eyes. Ophthalmology 2014;121:1350–8. [PubMed: 24629619]
8. Hitchings RA, Spaeth GL. The optic disc in glaucoma II: correlation of the appearance of the optic disc with the visual field. Br J Ophthalmol 1977;61:107–13. [PubMed: 843505]
9. Nicolela MT, Drance SM. Various glaucomatous optic nerve appearances: clinical correlations. Ophthalmology 1996;103:640–9. [PubMed: 8618765]
10. Broadway DC, Nicolela MT, Drance SM. Optic disk appearances in primary open-angle glaucoma. Surv Ophthalmol 1999;43 Suppl 1:S223–43. [PubMed: 10416767]
11. Sample PA, Girkin CA, Zangwill LM, et al. The African Descent and Glaucoma Evaluation Study (ADAGES): design and baseline data. Arch Ophthalmol 2009;127:1136–45. [PubMed: 19752422]
12. Ekici E, Moghimi S, Bowd C, et al. Capillary Density Measured by Optical Coherence Tomography Angiography in Glaucomatous Optic Disc Phenotypes. Am J Ophthalmol 2020;219:261–270. [PubMed: 32561168]
13. Leite MT, Rao HL, Weinreb RN, et al. Agreement among spectral-domain optical coherence tomography instruments for assessing retinal nerve fiber layer thickness. Am J Ophthalmol 2011;151:85–92 e1. [PubMed: 20970108]
14. Laird NM, Ware JH. Random-effects models for longitudinal data. Biometrics 1982;38:963–74. [PubMed: 7168798]
15. Laird NM, Donnelly C, Ware JH. Longitudinal studies with continuous responses. Stat Methods Med Res 1992;1:225–47. [PubMed: 1341659]
16. Zhang X, Dastiridou A, Francis BA, et al. Baseline Fourier-Domain Optical Coherence Tomography Structural Risk Factors for Visual Field Progression in the Advanced Imaging for Glaucoma Study. Am J Ophthalmol 2016;172:94–103. [PubMed: 27651070]
17. Medeiros FA, Meira-Freitas D, Lisboa R, Kuang TM, Zangwill LM, Weinreb RN. Corneal hysteresis as a risk factor for glaucoma progression: a prospective longitudinal study. Ophthalmology 2013;120:1533–40. [PubMed: 23642371]
18. Jammal AA, Thompson AC, Mariottoni EB, et al. Rates of Glaucomatous Structural and Functional Change From a Large Clinical Population: The Duke Glaucoma Registry Study. Am J Ophthalmol 2021;222:238–247. [PubMed: 32450065]
19. Tielsch JM, Sommer A, Katz J, Royall RM, Quigley HA, Javitt J. Racial variations in the prevalence of primary open-angle glaucoma. The Baltimore Eye Survey. JAMA 1991;266:369–74. [PubMed: 2056646]
20. Gordon MO, Beiser JA, Brandt JD, et al. The Ocular Hypertension Treatment Study: baseline factors that predict the onset of primary open-angle glaucoma. Arch Ophthalmol 2002;120:714–20; discussion 829-30. [PubMed: 12049575]
21. Heijl A, Leske MC, Bengtsson B, Bengtsson B, Hussein M, Early Manifest Glaucoma Trial G. Measuring visual field progression in the Early Manifest Glaucoma Trial. Acta Ophthalmol Scand 2003;81:286–93. [PubMed: 12780410]
22. Nouri-Mahdavi K, Hoffman D, Coleman AL, et al. Predictive factors for glaucomatous visual field progression in the Advanced Glaucoma Intervention Study. Ophthalmology 2004;111:1627–35. [PubMed: 15350314]
23. Albon J, Purslow PP, Karwatowski WS, Easty DL. Age related compliance of the lamina cribrosa in human eyes. Br J Ophthalmol 2000;84:318–23. [PubMed: 10684845]
24. Albon J, Karwatowski WS, Easty DL, Sims TJ, Duance VC. Age related changes in the non-collagenous components of the extracellular matrix of the human lamina cribrosa. Br J Ophthalmol 2000;84:311–7. [PubMed: 10684844]
25. Kotecha A, Izadi S, Jeffery G. Age-related changes in the thickness of the human lamina cribrosa. Br J Ophthalmol 2006;90:1531–4. [PubMed: 16943226]

26. Grunwald JE, Piltz J, Patel N, Bose S, Riva CE. Effect of aging on retinal macular microcirculation: a blue field simulation study. Invest Ophthalmol Vis Sci 1993;34:3609–13. [PubMed: 8258519]
27. Harris A, Harris M, Biller J, et al. Aging affects the retrobulbar circulation differently in women and men. Arch Ophthalmol 2000;118:1076–80. [PubMed: 10922201]
28. Burgoyne CF, Downs JC. Premise and prediction-how optic nerve head biomechanics underlies the susceptibility and clinical behavior of the aged optic nerve head. J Glaucoma 2008;17:318–28. [PubMed: 18552618]
29. Sawada Y, Hangai M, Murata K, Ishikawa M, Yoshitomi T. Lamina Cribrosa Depth Variation Measured by Spectral-Domain Optical Coherence Tomography Within and Between Four Glaucomatous Optic Disc Phenotypes. Invest Ophthalmol Vis Sci 2015;56:5777–84. [PubMed: 26325416]
30. Nicolela MT, Walman BE, Buckley AR, Drance SM. Various glaucomatous optic nerve appearances. A color Doppler imaging study of retrobulbar circulation. Ophthalmology 1996;103:1670–9. [PubMed: 8874441]
31. Spaeth GL. A new classification of glaucoma including focal glaucoma. Surv Ophthalmol 1994;38 Suppl:S9–17. [PubMed: 7940153]
32. Broadway DC, Drance SM. Glaucoma and vasospasm. Br J Ophthalmol 1998;82:862–70. [PubMed: 9828767]
33. Takada N, Omodaka K, Kikawa T, et al. OCT-Based Quantification and Classification of Optic Disc Structure in Glaucoma Patients. PLoS One 2016;11:e0160226. [PubMed: 27557112]
34. Healey PR, Mitchell P. Presence of an optic disc notch and glaucoma. J Glaucoma 2015;24:262–6. [PubMed: 20616749]
35. You JY, Park SC, Su D, Teng CC, Liebmann JM, Ritch R. Focal lamina cribrosa defects associated with glaucomatous rim thinning and acquired pits. JAMA Ophthalmol 2013;131:314–20. [PubMed: 23370812]
36. Arend O, Plange N, Sponsel WE, Remky A. Pathogenetic aspects of the glaucomatous optic neuropathy: fluorescein angiographic findings in patients with primary open angle glaucoma. Brain Res Bull 2004;62:517–24. [PubMed: 15036566]
37. Downs JC, Roberts MD, Burgoyne CF. Mechanical environment of the optic nerve head in glaucoma. Optom Vis Sci 2008;85:425–35. [PubMed: 18521012]
38. Marcus MW, de Vries MM, Junoy Montolio FG, Jansonius NM. Myopia as a risk factor for open-angle glaucoma: a systematic review and meta-analysis. Ophthalmology 2011;118:1989–1994 e2. [PubMed: 21684603]
39. Ren R, Wang N, Li B, et al. Lamina cribrosa and peripapillary sclera histomorphometry in normal and advanced glaucomatous Chinese eyes with various axial length. Invest Ophthalmol Vis Sci 2009;50:2175–84. [PubMed: 19387083]
40. Tan NY, Koh V, Girard MJ, Cheng CY. Imaging of the lamina cribrosa and its role in glaucoma: a review. Clin Exp Ophthalmol 2018;46:177–188. [PubMed: 29214709]
41. Sawada Y, Araie M, Ishikawa M, Yoshitomi T. Multiple Temporal Lamina Cribrosa Defects in Myopic Eyes with Glaucoma and Their Association with Visual Field Defects. Ophthalmology 2017;124:1600–1611. [PubMed: 28551164]
42. Sung MS, Kang YS, Heo H, Park SW. Optic Disc Rotation as a Clue for Predicting Visual Field Progression in Myopic Normal-Tension Glaucoma. Ophthalmology 2016;123:1484–93. [PubMed: 27157844]
43. Han JC, Han SH, Park DY, Lee EJ, Kee C. Clinical Course and Risk Factors for Visual Field Progression in Normal-Tension Glaucoma With Myopia Without Glaucoma Medications. Am J Ophthalmol 2020;209:77–87. [PubMed: 31493404]
44. Lloyd MJ, Mansberger SL, Fortune BA, et al. Features of optic disc progression in patients with ocular hypertension and early glaucoma. J Glaucoma 2013;22:343–8. [PubMed: 23719180]
45. Deokule SP, Doshi A, Vizzeri G, et al. Relationship of the 24-hour pattern of intraocular pressure with optic disc appearance in primary open-angle glaucoma. Ophthalmology 2009;116:833–9. [PubMed: 19195707]

46. Nakazawa T, Fuse N, Omodaka K, Aizawa N, Kuwahara S, Nishida K. Different types of optic disc shape in patients with advanced open-angle glaucoma. Jpn J Ophthalmol 2010;54:291–5. [PubMed: 20700795]
47. Schor KS, De Moraes CG, Teng CC, Tello C, Liebmann JM, Ritch R. Rates of visual field progression in distinct optic disc phenotypes. Clin Exp Ophthalmol 2012;40:706–12. [PubMed: 22429789]
48. Nakazawa T, Shimura M, Ryu M, et al. Progression of visual field defects in eyes with different optic disc appearances in patients with normal tension glaucoma. J Glaucoma 2012;21:426–30. [PubMed: 22314251]
49. Shin HY, Park HY, Jung Y, Choi JA, Park CK. Glaucoma diagnostic accuracy of optical coherence tomography parameters in early glaucoma with different types of optic disc damage. Ophthalmology 2014;121:1990–7. [PubMed: 24935284]
50. Omodaka K, Takada N, Yamaguchi T, Takahashi H, Araie M, Nakazawa T. Characteristic correlations of the structure-function relationship in different glaucomatous disc types. Jpn J Ophthalmol 2015;59:223–9. [PubMed: 25860862]
51. Medeiros FA, Zangwill LM, Bowd C, Vessani RM, Susanna R Jr., Weinreb RN. Evaluation of retinal nerve fiber layer, optic nerve head, and macular thickness measurements for glaucoma detection using optical coherence tomography. Am J Ophthalmol 2005;139:44–55. [PubMed: 15652827]
52. Hood DC, Wang DL, Raza AS, de Moraes CG, Liebmann JM, Ritch R. The locations of circumpapillary glaucomatous defects seen on frequency-domain OCT scans. Invest Ophthalmol Vis Sci 2013;54:7338–43. [PubMed: 24135758]
53. Hood DC. Improving our understanding, and detection, of glaucomatous damage: An approach based upon optical coherence tomography (OCT). Prog Retin Eye Res 2017;57:46–75. [PubMed: 28012881]
54. Takada N, Omodaka K, Nakazawa T. Regional susceptibility of the optic disc to retinal nerve fiber layer thinning in different optic disc types of eyes with normal tension glaucoma. Clin Exp Ophthalmol 2015;43:291–3. [PubMed: 25196307]
55. Diniz-Filho A, Abe RY, Zangwill LM, et al. Association between Intraocular Pressure and Rates of Retinal Nerve Fiber Layer Loss Measured by Optical Coherence Tomography. Ophthalmology 2016;123:2058–65. [PubMed: 27554036]
56. Iwase A, Araie M, Kuwayama Y, Murata H, Yamamoto T. Frequencies of 4 Distinct Patterns of Glaucomatous Disc Appearance and Their Clinical Associations in Japanese Population-based Studies. J Glaucoma 2019;28:487–492. [PubMed: 30882770]

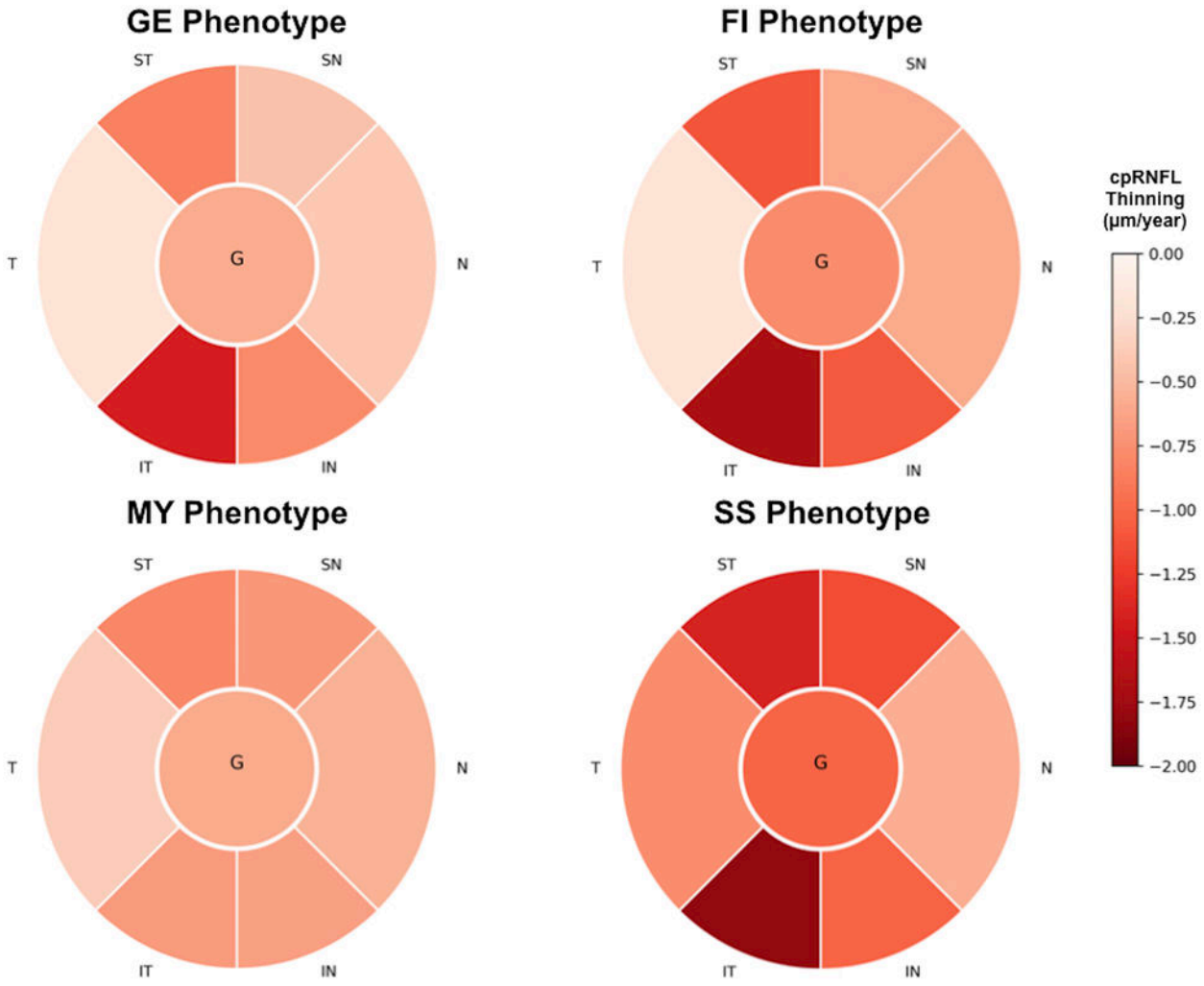

Figure 1.

Diagrams showing estimated mean rates of circumpapillary retinal nerve fiber layer (cpRNFL) thinning for generalized cup enlargement (GE), focal ischemic (FI), myopic glaucomatous (MY) and senile sclerotic (SS) eyes in early glaucoma. Data are presented as cpRNFL change rate (µm/year).

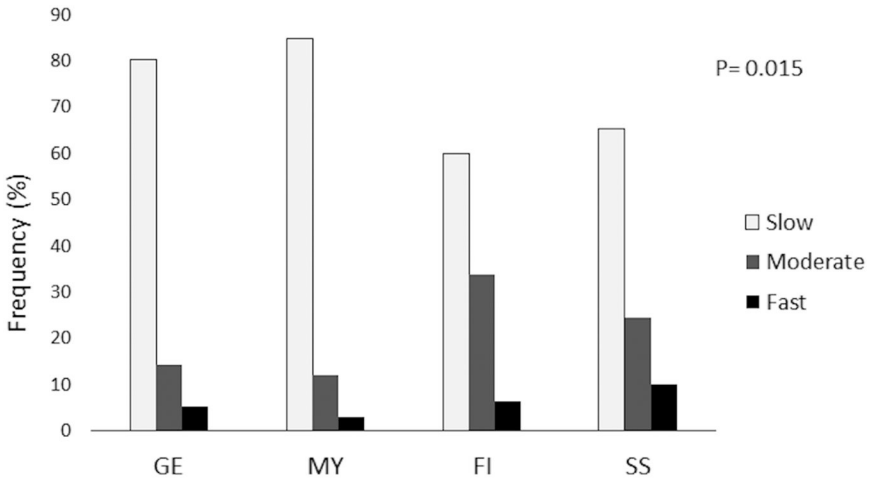

Figure 2.

Frequency of eyes classified as slow, moderate, and fast progressors according to pre-established range of mean rates of global circumpapillary retinal nerve fiber layer (cpRNFL) thinning for generalized cup enlargement (GE), focal ischemic (FI), myopic glaucomatous (MY) and senile sclerotic (SS) eyes in early glaucoma.

Table 1.

Demographics and Baseline Clinical Characteristics of Subjects

	GE	FI	MY	SS	*p* value
By Subject (No.)	61	46	18	48	
Age (years)	66.8 (64.3, 69.3)	66.2 (63.3, 69.2)	63.3 (58.9, 67.6)	74.3 (71.4, 77.2)	**<0.001** *§¶#*
Gender (M/F)	30/31	17/29	5/13	23/25	0.215
Race Non-African American/ African American	28/33	30/16	13/5	36/12	**0.001** *†‡§*
Self-reported HTN, n (%)	41 (67.2%)	24 (52.2%)	13 (72.2%)	33 (68.8%)	0.235
Self-reported DM, n (%)	18 (29.5%)	4 (8.7%)	7 (38.9%)	9 (18.8%)	**0.004** *†‖*
By Eye (No.)	76	53	22	67	
Axial Length (mm)	23.8 (23.6, 24.0)	23.9 (23.7, 24.2)	24.6 (24.1, 25.1)	24.0 (23.7, 24.2)	0.051 *‡‖*
CCT (μm)	530.0 (519.5, 540.5)	531.9 (519.3, 544.5)	545.5 (522.4, 568.5)	550.0 (537.2, 562.8)	0.160 *§*
Baseline IOP (mmHg)	14.6 (13.7, 15.6)	14.9 (13.7, 16.1)	15.7 (13.7, 17.7)	15.7 (14.5, 16.9)	0.606
Mean IOP (mmHg)	14.4 (14.2, 14.7)	13.7 (13.4, 14.0)	15.0 (14.4, 15.5)	15.2 (14.9, 15.4)	0.251
Baseline 24-2 MD (dB)	−1.4 (−1.8, −1.0)	−2.7 (−3.2, −2.2)	−1.3 (−2.1, −0.5)	−2.3 (−2.8, −1.9)	**<0.001** *†$‖#*
Baseline global cpRNFL (μm)	83.7 (80.3, 87.1)	73.4 (70.2, 76.5)	79.4 (74.9, 83.9)	72.6 (69.6, 75.5)	**<0.001** *†$‖#*
Follow-up (years)	5.9 (5.8, 6)	6.0 (5.8, 6.1)	6.1 (5.9, 6.2)	5.6 (5.5, 5.7)	0.572
Number of SDOCT Follow-up Scans	10.5 (10.3, 10.8)	10.9 (10.5, 11.3)	11.6 (11.1, 12.2)	11.6 (11.3, 11.9)	0.627

CCT = central corneal thickness; cpRNFL = circumpapillary retinal nerve fiber layer; dB = decibel; DM = diabetes mellitus; F = female; FI = focal ischemic; GE = generalized cup enlargement; HTN = hypertension; IOP = intraocular pressure; M = male; MD = mean deviation; MY = myopic glaucomatous; SDOCT = spectral-domain optical coherence tomography; SS = senile sclerotic. Values are shown in mean (95% confidence interval), unless otherwise indicated. Statistically significant *p* values shown in bold.

Tukey honestly significant difference test $p<0.05$ for:

†GE vs. FI

‡GE vs MY

§GE vs SS

$^{\|}$MY vs FI

¶SS vs FI

$^{\#}$SS vs MY.

Table 2.

Comparison of Rates of cpRNFL Thinning among Glaucomatous Optic Disc Phenotypes in Early Glaucoma

	GE	FI	MY	SS	*p* value (adjusted)
Global cpRNFL Change Rate (μm/year)					
Mean Global	−0.58 (−0.75, −0.40)	−0.77 (−0.97, −0.57)	−0.59 (−0.81, −0.36)	−1.01 (−1.30, −0.73)	**<0.001** *§#* **(<0.001)** *§#*
Regional cpRNFL Change Rate (μm/year)					
Temporal	−0.20 (−0.37, −0.04)	−0.20 (−0.50, 0.11)	−0.37 (−0.70, −0.05)	−0.76 (−1.05, −0.47)	**0.002** *§¶* **(0.042)** *§¶*
Nasal	−0.40 (−0.69, −0.11)	−0.59 (−0.92, −0.25)	−0.54 (−0.89, −0.19)	−0.57 (−0.88, −0.26)	0.118 **(0.010)** *§*
Superior temporal	−0.84 (−1.17, −0.52)	−1.10 (−1.52, −0.68)	−0.80 (−1.30, −0.30)	−1.40 (−1.86, −0.93)	**0.003** *§* **(0.074)**
Superior nasal	−0.44 (−0.75, −0.13)	−0.60 (−0.92, −0.27)	−0.71 (−1.16, −0.26)	−1.15 (−1.54, −0.77)	**0.012** *§¶* **(0.042)** *§¶*
Inferior temporal	−1.43 (−1.84, −1.01)	−1.68 (−2.21, −1.14)	−0.68 (−1.10, −0.26)	−1.82 (−2.33, −1.31)	**0.002** *‖#* **(0.003)** *‖#*
Inferior nasal	−0.78 (−1.09, −0.46)	−1.08 (−1.43, −0.73)	−0.66 (−1.10, −0.21)	−1.03 (−1.45, −0.62)	**0.001** **(<0.001)** *#*

cpRNFL = circumpapillary retinal nerve fiber layer; FI = focal ischemic; GE = generalized cup enlargement; MY = myopic glaucomatous; SS = senile sclerotic. Values are shown in mean (95% confidence interval), unless otherwise indicated.

Statistically significant *p* values shown in bold.

Tukey honestly significant difference test $p<0.05$ for:

†GE vs. FI

‡GE vs MY

§GE vs SS

$^{\|}$MY vs FI

¶SS vs FI

$^{\#}$SS vs MY.

Table 3.

Factors Contributing to the Rate of cpRNFL Thinning Over Time in Early Glaucoma Eyes by Univariable and Multivariable Mixed Model Analysis

	Univariable		Multivariable	
	β, 95 % CI	***p* value**	**β, 95 % CI**	***p* value**
Age, per 10 years older	0.07 (−0.05, 0.18)	0.262	0.10 (−0.03, 0.22)	0.146
Gender: M/F	−0.05 (−0.29, 0.19)	0.696		
Race:Non-African American / African American	−0.06 (−0.30, 0.19)	0.654	−0.03 (−0.29, 0.22)	0.787
Self-reported HTN	0.20 (−0.05, 0.45)	0.122		
Self-reported DM	0.22 (−0.05, 0.49)	0.111		
Axial length, per 1mm longer	0.003 (−0.12, 0.13)	0.958		
CCT, per 10μm thinner	−0.01 (−0.03, 0.02)	0.617		
Mean IOP, per mmHg higher	−0.08 (−0.11, −0.04)	**<0.001**	−0.07 (−0.11, −0.03)	**<0.001**
Baseline 24-2 MD, per 1 dB worse	−0.02 (−0.08, 0.05)	0.623	−0.01 (−0.07, 0.06)	0.878
Phenotypes		**<0.001**		**0.014**
SS vs GE	−0.43 (−0.72, −0.15)	**0.003**	−0.50 (−0.83, −0.18)	**0.002**
SS vs FI	−0.23 (−0.54, 0.09)	0.158	−0.24 (−0.57, 0.10)	0.169
SS vs MY	−0.43 (−0.85, −0.02)	**0.041**	−0.58 (−1.02, −0.14)	**0.010**

CCT = central corneal thickness; cpRNFL = circumpapillary retinal nerve fiber layer; dB = decibel; DM = diabetes mellitus; F = female; FI = focal ischemic; GE = generalized cup enlargement; HTN = hypertension; IOP = intraocular pressure; M = male; MD = mean deviation; MY = myopic glaucomatous; SS = senile sclerotic. Values are shown in β coefficient (95% confidence interval), unless otherwise indicated. Statistically significant *p* values shown in bold.